Outlier Color Identification for Search and Rescue

Abhishek Gaur, Ashutosh Sanan

December 15, 2016

Boston University

Department of Electrical and Computer Engineering

BOSTON UNIVERSITY

Outlier Color Identification for Search and Rescue

Abhishek Gaur, Ashutosh Sanan

Boston University
Department of Electrical and Computer Engineering
8 Saint Mary's Street
Boston, Ma 02215
www.bu.edu/ece

Table of Contents

Problem Statement

The use of Unmanned Aerial Vehicles for the task of search and rescue is fast growing owing to the high-quality imaging capabilities of the drones and ease of navigation. The task is analogous to anomaly detection in hyperspectral images. Hyperspectral imaging systems, unlike conventional images, employs an imaging spectrometer to detect and extract information in many spectral bands. The spectral information generally includes the visible and infrared regions of the electromagnetic spectrum.

Anomaly detection [1] is the ability to find spectral outliers within a complex background in a scene with no priori information about the scene or its specific contents. The same technique applies for outlier color detection for search and rescue.

Literature Survey

There has been a lot of work on anomaly detection on hyperspectral images and videos. Most of it was focused on anomaly detection in videos in which both temporal and non-temporal information is used for prediction whereas our work is only concerned with color values/non-temporal information of the image. Therefore, our research is focused on anomaly detection in hyperspectral images.

The most popular technique used is Reed-Xiaoli Detector [2], often considered as benchmark in this field, which computes the similarity of each pixel to its neighboring or global statistics under the assumption that the spectral data is distributed according to multivariate Gaussian distribution. There are also various variations of the same [3].

Another approach is to use color histograms. Rasmussen et al. [4] use hue histogram and local saliency measure to find unusually colored objects and then enhance the frame to draw observer's attention towards the anomaly.

Another class of detection algorithm is region-based detection [5] in which pixels are grouped into clusters based on a criteria and then figure out if the cluster is an anomaly or normal pixel. One of the approach is k-Means based detection [6], in which the clusters are made based on distance of a point from the centroid of each cluster. After k-Means outlier centroid detection is applied which predicts which of the centroid corresponds to an anomaly. The output image of it can be considered as a Markov Random field to incorporate the spatial correlation between the pixels to improve the results [7].

Dataset

We found few videos online for Drone Search and Rescue but the subject of interest (people to be rescued) were very hard to locate due to them wearing indistinctive clothes with respect to the surroundings.

Hence, we fabricated our own dataset by blending different colored blobs on the drone footage shots. The dataset consists of 15 images covering different scenarios from best to worst test performance.

Color Space

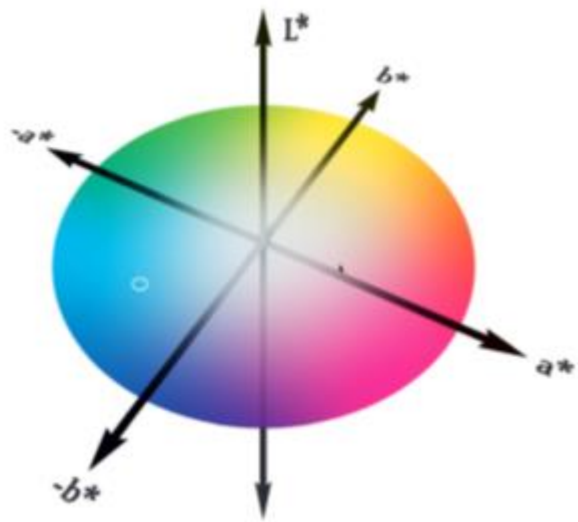

*Figure 1: L*a*b* color space*

We use L*A*B color space for all our image analysis. This color space defined by the CIE based on one channel for Luminance (lightness) (L)and two color channels (a and b). In this color space, a difference between green and greenish-yellow is relatively large, whereas the distance distinguishing blue and red is quite small. In this model, the color differences which you perceive correspond to distances when measured colorimetrically. The a axis extends from green (-a) to red (+a) and the b axis from blue (-b) to yellow (+b). The brightness(L) increases from the bottom to the top of the three-dimensional model.

This color space is better suited to many digital image manipulations than the RGB space, which is typically used in image editing programs. The *L*a*b** color space includes all perceivable colors, which means that its gamut exceeds those of the RGB and CMYK color models. One of the most important attributes of the *L*a*b**-model is device independence. This means that the colors are defined independent of their nature of creation or the device they are displayed on. The *L*a*b** color space is used when graphics for print have to be converted from RGB to CMYK, as the *L*a*b** gamut includes both the RGB and CMYK gamut. Also it is used as an interchange format between different devices as for its device independency. The space itself is a three-dimensional real number space, that contains an infinite number of possible representations of colors including colors outside human vision.

Algorithms Implemented:

Reed-Xiaoli Anomaly Detector

The benchmark in hyperspectral anomaly detection is the RX algorithm, developed by Reed and Yu[1]. In this approach, the assumption is made that a normal pixel is drawn from a Multivariate Gaussian distribution specified by $N(\mu,\Sigma)$. We develop a threshold test to classify each pixel under the following hypothesis:

Null Hypothesis H_0: $X \approx N(\mu,\Sigma)$

The pixels that follow the normal distribution follow this hypothesis.

Alternate Hypothesis H_1: $X \approx$ Uniform (C)

The pixels that do not follow the normal distribution follow this hypothesis.

The log-likelihood function is used to maximize the probability of detecting an anomaly when an anomaly exists for a fixed rate of false alarm which is controlled by the threshold T.

$$f(x) = \log \frac{p(x:H1)}{p(x:H0)} \gtrless T$$

Expanding the above equation, we get:

$$f(x) = \log p(x:H_1) - \log p(x:H_0) = \log c - \log p(x:H_0) \gtrless T$$

Assuming that x is n n-dimensional vector, the above equation can be written as:

$$f(x) = \log c + \frac{n}{2}\log(2\pi) + \frac{1}{2}\log|\Sigma| + \frac{1}{2}\left((x-\mu)^T\,\Sigma^{-1}\,(x-\mu)\right) \gtrless T$$

The constants and multiplicative factor can be grouped as into a new threshold S to yield he Mahalanobis distance between the pixel and the background region with the form:

$$(x-\mu)^T\,\Sigma^{-1}\,(x-\mu) \gtrless ▯$$

where,

x: target feature vector

μ: mean of background region

Σ: covariance matrix of background region

S: threshold

DWEST

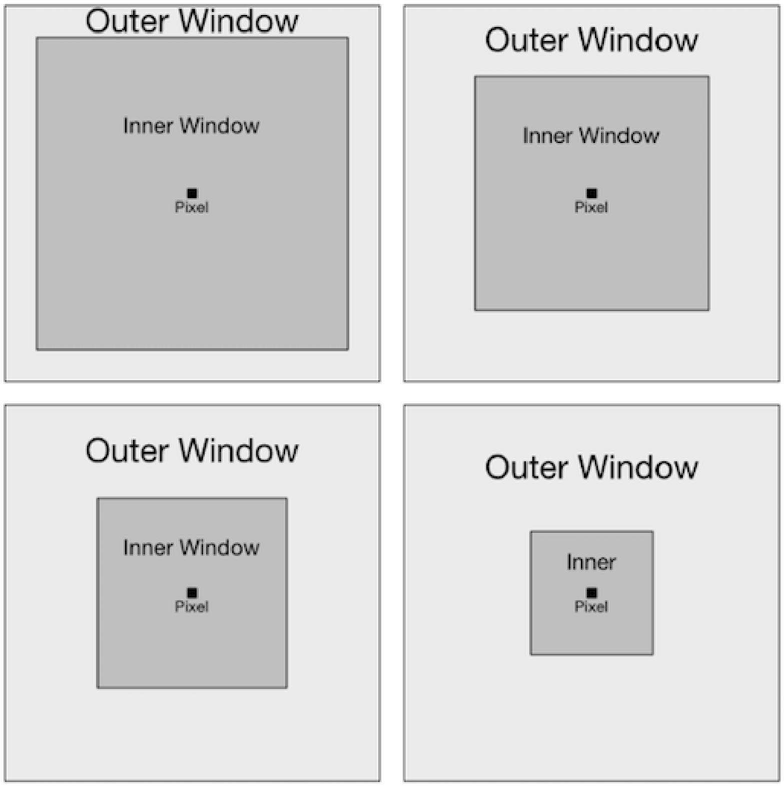

Figure 2: Windowing Technique for DWEST Algorithm.

Dual window-based eigen separation transform (DWEST) is an adaptive algorithm which is similar to RX detector, and similarly uses covariance to compare the material differences between an inner and outer window. The key difference between them is that DWEST used the differential covariance matrix calculated as:

$\mathbf{K}_{diff} = \mathbf{K}_{inner} - \mathbf{K}_{outer}$

where $\mathbf{K}_{inner}$ is the covariance matrix of the inner window and $\mathbf{K}_{outer}$ is the covariance matrix of the outer window. The small subset of the eigenvalues in the $\mathbf{K}_{diff}$ which will have positive values, and their corresponding eigenvectors ($\mathbf{V}_i$), will correspond to distinctive, differential data structures and can be used to project the mean difference between the windows. This suppresses the background from the outer window.

To experiment some variation, we implemented a muti-window DWEST technique where individual detectors are analyzed for different window sizes[2]. Figure 1 illustrates the implementation with multiple inner window sizes. The final detector represents the maximum of the above mentioned individual detectors:

$$\delta_{\mathrm{MW-DWEST}} = \max_{i=1,\dots,N} \left\{ \delta^{(i)}_{\mathrm{DWEST}}(\mathbf{u}[\mathbf{x}]) \right\}$$

For the experimentation, we have evaluated the outer window size of 11x11 and 15x15 with inner window sizes of 1x1, 3x3, 5x5 and 7x7.

NSWTD

A great challenge of hyperspectral target detection is to detect subtle targets without prior knowledge, particularly, when the targets of interest are insignificant and occur with low probabilities.
A relatively new anomaly detection technique is nested spatial window-based target detection (NSWTD) approach for hyperspectral imagery where a set of different spatial windows are nested and implemented to extract targets whose signatures are spectrally and spatially distinct [5]. The use of nested spatial windows is determined by the image pixel resolution and applications.

This technique uses a technique called Orthogonal Subspace Projection (OSP)[6]:

$$\mathbf{P}_{\mathbf{s}}^{\perp} = \mathbf{I} - \mathbf{s}(\mathbf{s}^T\mathbf{s})^{-1}\mathbf{s}^T$$

This is used because OSP projects a vector into a new space which optimally minimizes the background signal. This can be shown as below. Consider the signal be a linear combination of required signal (**v[x]**) and background (**s[x]**):

$$\begin{aligned}
\mathbf{u}[\mathbf{x}] &= \mathbf{v}[\mathbf{x}] + \mathbf{s}[\mathbf{x}] \\
\mathbf{P}_{\mathbf{s}}^{\perp}\mathbf{u} &= \mathbf{P}_{\mathbf{s}}^{\perp}\mathbf{v} + \mathbf{P}_{\mathbf{s}}^{\perp}\mathbf{s} \\
&= \mathbf{P}_{\mathbf{s}}^{\perp}\mathbf{v} + (\mathbf{I} - \mathbf{s}(\mathbf{s}^T\mathbf{s})^{-1}\mathbf{s}^T)\mathbf{s} \\
&= \mathbf{P}_{\mathbf{s}}^{\perp}\mathbf{v} + \mathbf{s} - \mathbf{s} \\
&= \mathbf{P}_{\mathbf{s}}^{\perp}\mathbf{v}
\end{aligned}$$

Using Orthogonal Subspace Projection, we can calculate a measure called Orthogonal Projection Divergence.

$$\mathrm{OPD}(\mathbf{s}_i, \mathbf{s}_j) = \sqrt{\mathbf{s}_i^T P_{\mathbf{s}_j}^{\perp} \mathbf{s}_i + \mathbf{s}_j^T P_{\mathbf{s}_i}^{\perp} \mathbf{s}_j}$$

It denotes the spectral differences between two signals and can be used compare spectral differences between two windows in an image. This algorithm also works in a similar manner as DWEST.

Similar to DWEST, windowing is done in the similar manner with multiple inner window sizes. The same window sizes were used as DWEST.

MW-NSWTD

A variation of NSWTD, Multi Window-NSWTD does the same thing but now does the comparison between three distinct windows. The outermost window is used for whitening (background suppression), and then classifies pixels as an anomaly based on the difference between the inner and the outer window.

$$\delta_{\mathrm{MW-NSWTD}}(\mathbf{u}[\mathbf{x}]) = \sqrt{\mu_{\mathrm{inner}}[\mathbf{x}]^T P^{\perp}_{\mu_{\mathrm{outer}}[\mathbf{x}]} \mu_{\mathrm{inner}}[\mathbf{x}] + \mu_{\mathrm{middle}}[\mathbf{x}]^T P^{\perp}_{\mu_{\mathrm{outer}}[\mathbf{x}]} \mu_{\mathrm{middle}}[\mathbf{x}]}$$

The above equation is same as Orthogonal Projection Divergence defined in the method above but with a slight variation. It used Orthogonal Subspace Projection calculated from the outer window to calculate the divergence between inner and middle window.

The windowing technique is shown below:

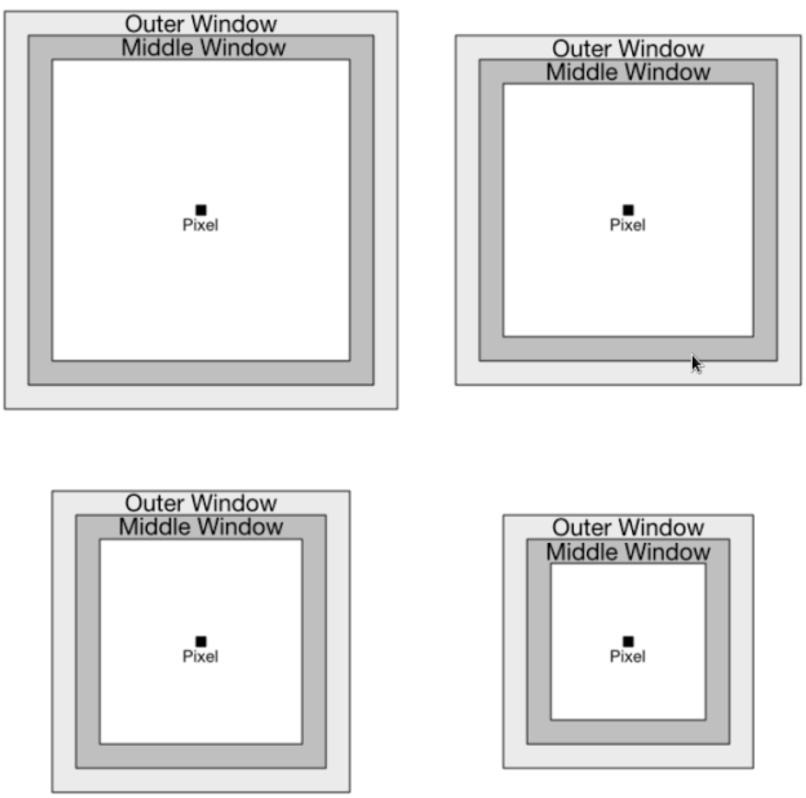

Figure 3: Windowing Technique for MW-NSWTD Algorithm.

Experimental Results and Conclusion:

We obtained very good results with Reed-Xiaoli Anomaly Detector and DWEST Detector. We used it as a benchmark for evaluating the performance of NSWTD and MW-NSWTD. From the results, we concluded that MW-NSWTD performs the best in terms of finding an outlying element in the image.

That said, there was a clear trade-off in terms of computation complexity and accuracy in the four algorithms. The former two (RXD and DWEST) performed the computation faster than the latter two (NSWTD and MW-NSWTD) but were less accurate than them on multiple occasions.

It was worth noting that even though there was a performance difference among different algorithms, all four of them are very slow in general and take a long time for computation (of the order of ~500 seconds/image). This limitation renders the system useless since for the purpose of search and rescue, the system should be running real-time. The embedded systems deployed in these drones does not have enough computational power to be able to perform these operations in real time.

There were a few cases where the background clutter was too much and the image was not very high resolution in case of which the results were non-informative in all algorithms.

Fig 4: Test image with good results

Fig 4.1 : RXD output

Fig 4.2 : DWEST Output

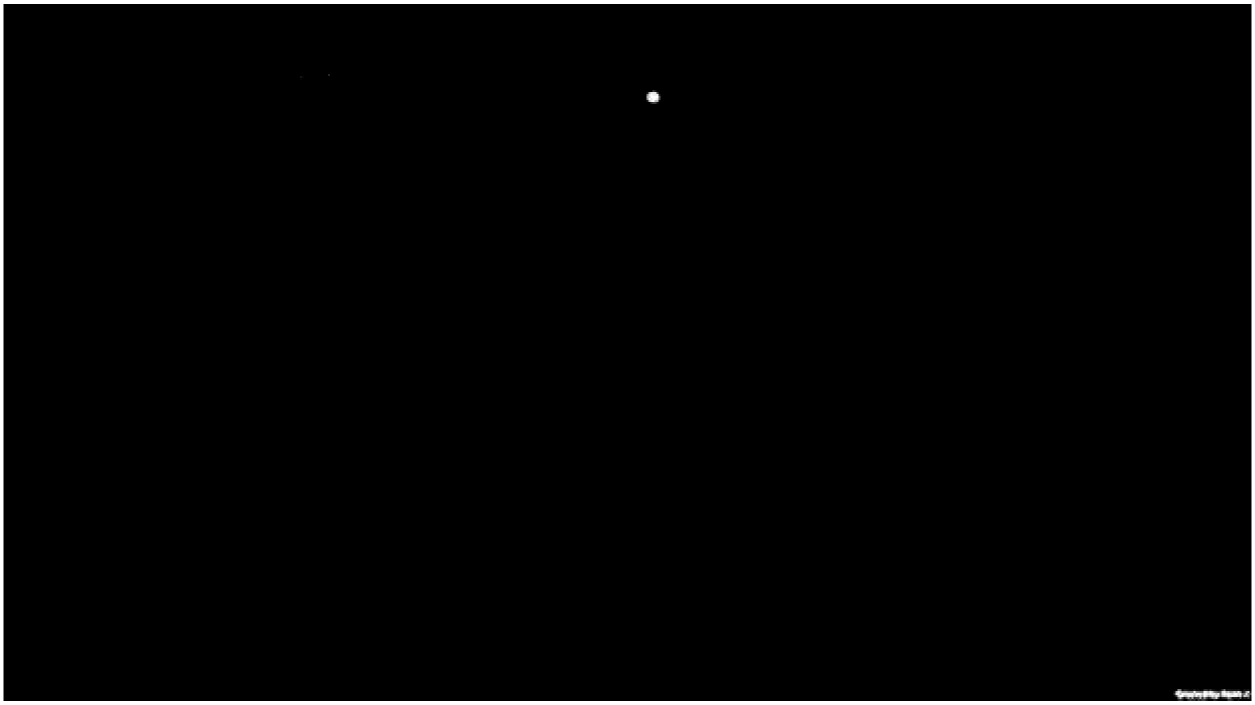

Fig 4.3 : NSWTD Output

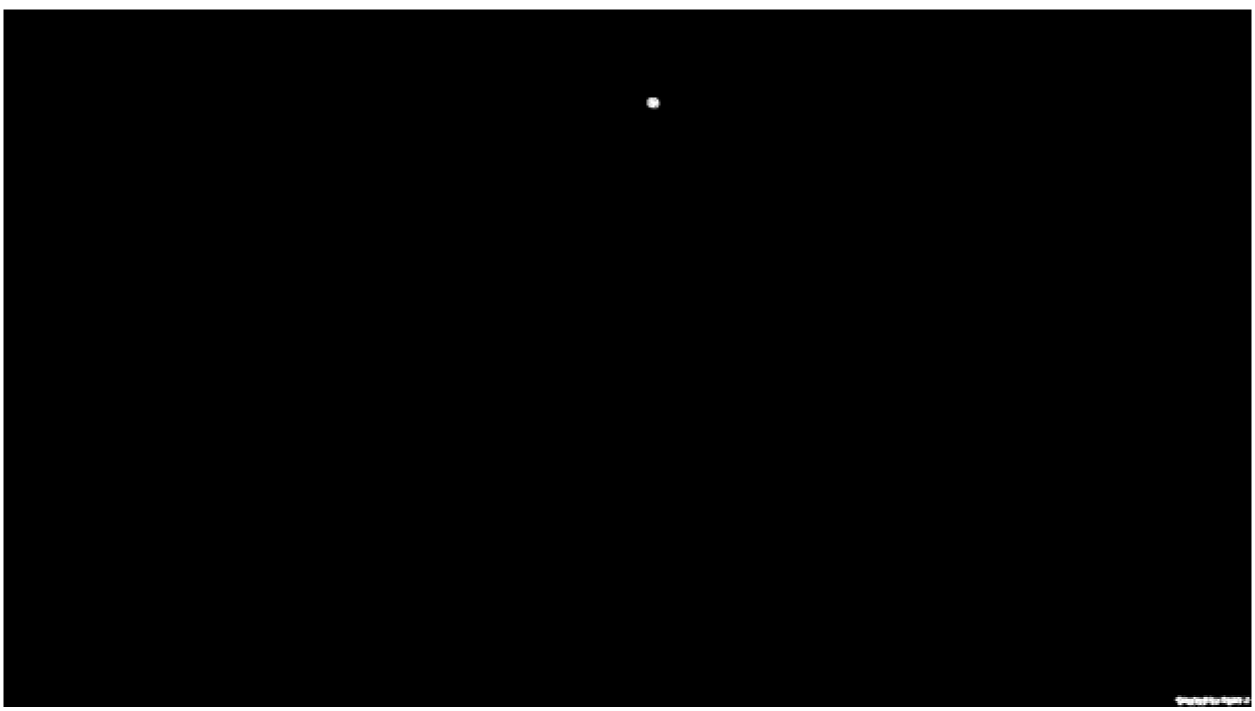

Fig 4.4 : MW-NSWTD Output

Fig 5 : Test Image with bad results

Fig 5.1: RXD Output

Fig 5.2: DWEST Output

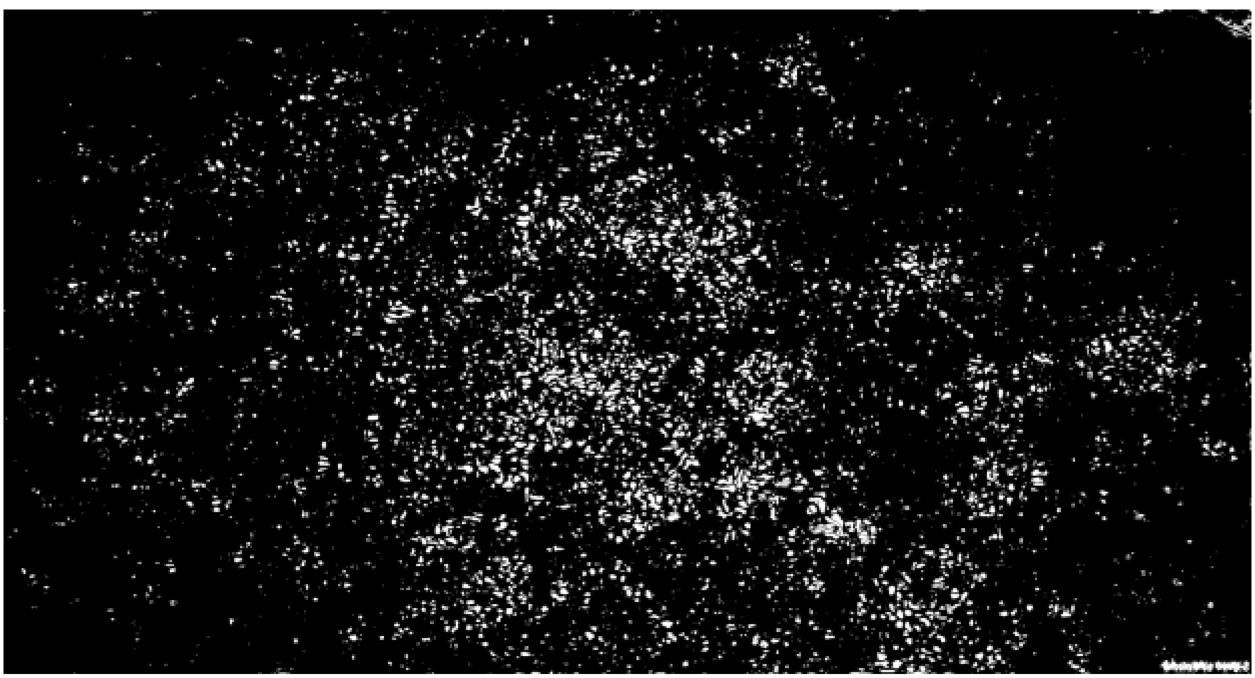

Fig 5.3 : NSWTD Output

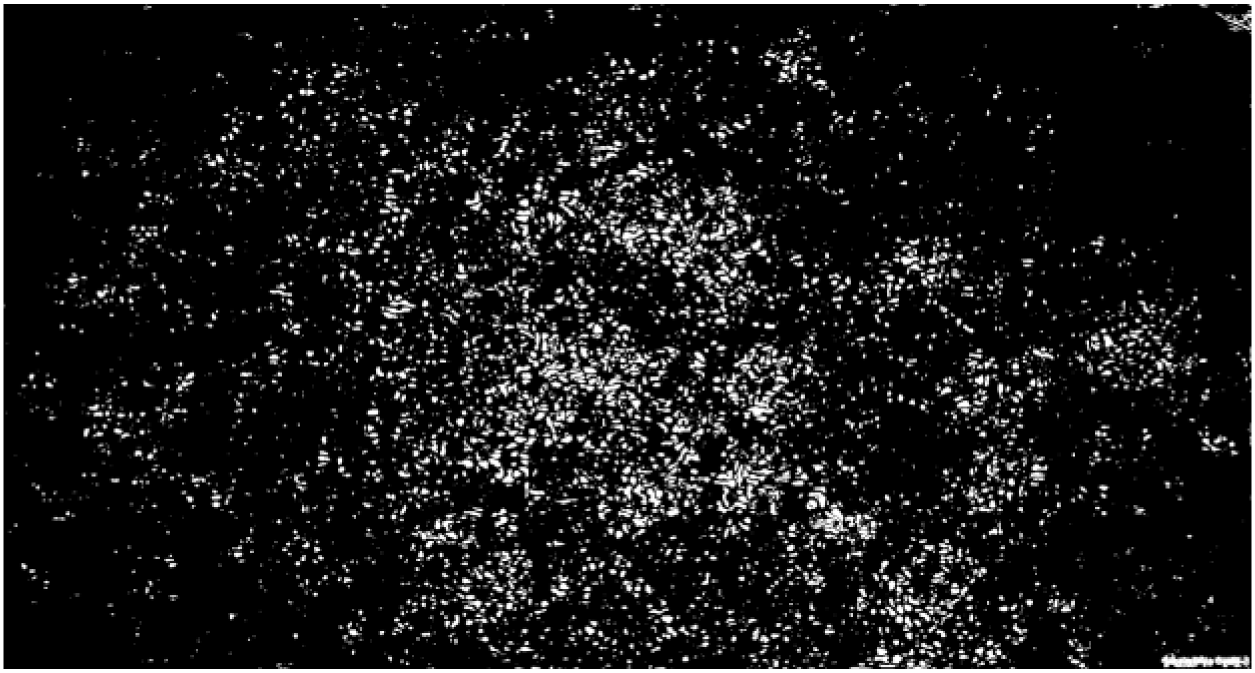

Fig 5.4 : MW-NSWTD Output

References:

[1] I. Reed and X. Yu, "Adaptive multiple-band CFAR detection of an optical pattern with unknown spectral distribution, "IEEE Transactions on Acoustic, Speech and Signal Processing, vol. 38, no. 10, pp. 1760-1770, 1990.

[2] W.-M. Liu and C.-I. Chang, Multiple-Window Anomaly Detection for Hyper-spectral Imagery,"IEEE Journal of Selected Topics in Applied Earth Observations and Remote Sensing, vol. 6, pp. 644{658, May 2013}

[3] Tapas Kanungo, Senior Member, IEEE, David M. Mount, Member, IEEE, “An Efficient k-Means Clustering Algorithm: Analysis and Implementation”.

[4] B. S. Morse, D. Thornton, and M. A. Goodrich,Color anomaly detection and suggestion for wilderness search and rescue. New York, New York, USA: ACM,Mar. 2012.

[5] D. Manolakis and D. Marden, Hyperspectral image processing for automatic target detection applications," Lincoln Laboratory . . ., 2003.

[6] T. E. Smetek and K. W. Bauer, Finding hyperspectral anomalies using multi-variate outlier detection,"Aerospace Conference, 2007.

[7] D. C. Borghys, V. Achard, S. R. Rotman, N. Gorelik, C. Perneel, Scwheicher, and Emile, Hyperspectral anomaly detection: a comparative evaluation of methods,"General Assembly and Scientific Symposium, XXXth URSI, pp. 14, Feb.2011.

[8] H. Kwon, Adaptive anomaly detection using subspace separation for hyperspectral imagery," Optical Engineering, vol. 42, pp. 3342{10, Nov. 2003.

[9] M. J. Carlotto, \A cluster-based approach for detecting man-made objects and changes in imagery," IEEE Transactions on Geoscience and Remote Sensing, vol. 43, pp. 374, 387, Jan. 2005.

[10] N. D. Rasmussen, D. R. Thornton, and B. S. Morse, Enhancement of unusual color in aerial video sequences for assisting wilderness search and rescue," 2008 15th IEEE International Conference on Image Processing, pp. 1356, 1359, 2008.

[11] T. Bolukbasi and P. Tran, Outlier color identi cation for search and rescue," BU Department of Electrical and Computer Engineering Technical Reports, Dec. 2012.

[12] C.-I. Chang, Orthogonal subspace projection (OSP) revisited: a comprehensive study and analysis," IEEE Transactions on Geoscience and Remote Sensing, vol. 43, pp. 502-518, Feb. 2005.